$$\psi_n(\xi) = \left(\frac{1}{\xi}\cdot\frac{d}{d\xi}\right)^n \frac{sh\xi}{\xi}$$

Finally, Ω is expressed as

$$\Omega = \frac{2B}{3\xi_1}$$

APPENDIX B. DERIVATION OF THE STRESS TENSOR AND OF THE YIELD CONDITION

Equation (4) together with boundary conditions (5) should be solved in order to obtain the stresses in the solid matrix, when deformation of the particle is neglected.

A mathematically complete solution of Equation (4) is the Boussinesq-Papkovitch-Neuber solution (Gurtin, 1972); the displacement field d is expressed as

$$\mathbf{d} = \Psi^\circ - \frac{1}{4(1-N)}\cdot\nabla(\mathbf{x}\cdot\Psi^\circ + \varphi) \qquad (B1)$$

where φ and Ψ° are scalar and vector fields that satisfy

$$\nabla^2\varphi = \frac{\mu}{mk}\cdot\mathbf{x}\cdot\tilde{\mathbf{u}} + \frac{(\rho_S-\rho_L)(1-\epsilon)gz}{m} \qquad (B2a)$$

$$\nabla^2\Psi^\circ = -\frac{\mu}{mk}\tilde{\mathbf{u}} - \frac{(\rho_S-\rho_L)(1-\epsilon)}{m}\cdot\mathbf{g} \qquad (B2b)$$

Particular solutions of these equations with second member can be easily found, since $\tilde{\mathbf{u}}$ satisfies Brinkman equation (1b) and $\tilde{p}$ is a harmonic field which can be expanded as a sum of solid spherical harmonics $\tilde{p}_n$. General solutions of the homogeneous equations are either a scalar or a vector harmonic field.

In the present case, that is, for $\tilde{p} = \tilde{p}_1$, the displacement field d can be expressed as (Love, 1927)

$$m\mathbf{d} = -\tilde{\mu\mathbf{u}} + \bar{A}\left(\frac{r^2}{3}\cdot\nabla\tilde{p}_1 - \tilde{p}_1\mathbf{x}\right) + \frac{\hat{\psi}_1}{6}\cdot\frac{H}{F}\cdot r^2\nabla\tilde{p}_1$$

$$-\frac{1}{4(1-N)}\cdot\nabla\left[\left(\frac{\hat{\psi}_1}{15}\cdot\frac{H}{F} - \frac{2}{3}\cdot\bar{A}\right)r^2\tilde{p}_1\right] \qquad (B3)$$

where $\bar{A}$ is determined by the boundary condition (5).

Two constants are generally necessary to determine the displacement field d (see Adler, 1978). But in the particular case of solid spherical harmonics of order 1, boundary conditions can be fulfilled with only one constant, since the total force exerted upon the porous solid matrix must be equal to the apparent weight of the porous particle.

The stress tensor is determined from (B3) and (3). Its deviatoric part is given by (9), where T is expressed as

$$T = \frac{H}{6F}\cdot(2\hat{\psi}_1 + \xi_1^2\hat{\psi}_3 - \hat{\psi}_2) \qquad (B4)$$

The coefficients which appear in the yield condition (10) are given by

$$\mathcal{L} = 2\xi^2\cdot\left(\psi_2 - \frac{\psi_1}{2} + \frac{F}{H}\cdot T\right)^2 \qquad (B5a)$$

$$\mathcal{M} = \frac{\psi_1^2}{2} + 9\psi_2^2 - 4\psi_1\psi_2 + \psi_3^2\xi^4 + 6\psi_2\psi_3\xi^2 - 2\psi_1\psi_3\xi^2 + \frac{2}{3}\cdot\frac{F}{H}\cdot T\cdot(4\psi_3\xi^2 + 2\psi_2 - \psi_1) + \frac{2}{3}\cdot\left(\frac{F}{H}\cdot T\right)^2 \qquad (B5b)$$

Manuscript received April 24, 1978; revision received January 22, and accepted February 6, 1979.

Quantitative Interpretation of Phase Volume Behavior of Multicomponent Systems Near Critical Points

PAUL D. FLEMING, III
and
JAMES E. VINATIERI
Phillips Petroleum Company
Bartlesville, Oklahoma

Equations describing phase volumes in multicomponent, multiphase systems in the neighborhood of critical points are derived to aid in the location of such critical points. The theory is in good agreement with experiments for three ternary systems and four surfactant systems of the type used for tertiary oil recovery.

SCOPE

The behavior of phase volumes of multicomponent systems in the neighborhood of critical points is indicative of the nearness to such points. Since interfacial tensions between the critical phases become vanishingly small near a critical point, location of critical points should prove beneficial in the design of tertiary oil recovery systems employing surfactants or high pressure gases.

A convenient way of representing the phase volumes of multicomponent systems is to employ phase volume diagrams. Such a diagram expresses the relative volumes of phases present in a series of samples whose overall compositions lie along some smooth path in the phase diagram. Modern theory of critical phenomena has been used to develop equations relating the shapes of phase volume diagrams to the proximity to critical points.

CONCLUSIONS AND SIGNIFICANCE

The theory is in good agreement with experiments in three ternary systems and in four surfactant systems of the type used in tertiary oil recovery. A three-parameter equation is sufficient to describe phase volume diagrams in two-phase, ternary systems, while three-phase systems with four or more components require a four-parameter equation. In both cases, one of the parameters directly measures the nearness of the particular path to a critical point. Since interfacial tensions approach zero as critical points are approached, trends in interfacial tensions can, therefore, be characterized solely from observations of phase volumes. This will reduce the number of interfacial tensions which need to be measured when surfactant systems are studied.

Recently, phase volume diagrams have been used to summarize conveniently the phase behavior of surfactant systems (Boneau and Clampitt, 1977; Vinatieri, 1977; Fleming et al., 1978). Such diagrams are obtained when the relative volumes of phases in a multicomponent system are plotted vs. some independent composition variable of the system. They have greatly facilitated the development of surfactant systems effective for tertiary oil recovery.

In order to appreciate fully the information contained in phase volume diagrams, it is necessary to determine the underlying physical phenomena which determine the shapes of these diagrams. The modern theory of critical phenomena (Stanley, 1971) has been especially concerned with the shapes of phase diagrams in the neighborhood of critical points. These shapes have been characterized in terms of a set of critical exponents which are universal in the sense that they are the same for all ordinary fluid-fluid critical points. These exponents are, in all cases, different from what would be predicted from classical theories in which the free energy is assumed to be an analytic function of the other thermodynamic variables. For example, the isothermal compressibility of a single-component system in the neighborhood of its critical point is of the form

$$K_T = -\frac{1}{V}\left(\frac{\partial V}{\partial P}\right)_T \propto (T - T_c)^{-\gamma} \qquad (1)$$

where γ is very close to 5/4 for all substances. This differs from the value for γ of unity obtained from the van der Waals equation, for example. The value is, within experimental error, the same as that for the three-dimensional Ising model (Hockner and Moldover, 1976; Greer 1976). The definitions and values of the critical exponents for liquid-vapor critical points are summarized in Table 1.

The shape of the binodal curve near the plait point in a ternary system has been studied experimentally by Zollweg (1971). He found that, within experimental error, the binodal curve in the system chloroform, water, and ethanol is locally of degree $d = (1 - \alpha)/\beta$. A value of $d = 2$ would have been expected if the curve were analytic. The result, $d = (1 - \alpha)/\beta$, was predicted by general theoretical arguments by Widom (1967) and Fisher (1968) and was verified within the context of a decorated lattice gas model by Clark and Neece (1968).

The results presented herein allow the analysis of the shapes of phase volume diagrams in the neighborhood of plait points. The resulting equations will be seen to give good fits to experimental phase volume diagrams in the ternary system water, chloroform, and acetone. The equations will then be generalized to apply to regions of three fluid phases in systems having more components. Good fits to experimental phase volume diagrams in three-phase surfactant systems will be obtained with the generalized equation.

One important result of the analysis presented here is that one of the parameters in the theory measures the distance from the path of the phase volume diagram to a critical point. The importance of the nearness to a critical point to oil recovery is clear once it is recalled that the interfacial tension between two fluid phases approaches zero as a critical point is approached. This allows the characterization of trends in interfacial tensions solely from observations of phase volumes and should make possible the derivation of a quantitative relationship between interfacial tension and phase volumes. This will reduce the number of interfacial tensions which need to be measured, although it will not entirely eliminate the need to measure interfacial tensions.

The equations for the phase-volume behavior of ternary systems are presented. Then, these equations will be compared with actual phase volume diagrams in ternary systems. Later the equations will be generalized to multicomponent, multiphase systems and compared with experimental phase volume diagrams in three-phase surfactant systems.

THEORY DERIVATION OF EQUATIONS FOR A TERNARY SYSTEM

Consider a ternary system in a two-phase region at constant temperature and pressure. From the phase rule, such a system possesses only 1 degree of freedom. If we label the components by i, $i = 1, 2, 3$, then we can express all thermodynamic quantities in terms of the chemical potential of a single component, for example, that of component 1, μ_1. From the theory of critical phenomena (Stanley, 1971), the difference between the concentrations of component 1 in the two phases must approach zero at the critical (plait) point according to

$$C_1 - \tilde{C}_1 = B_1 \epsilon_1^{\beta} \qquad (2)$$

where $\epsilon_1 = |(\mu_1 - \mu_1^C)/\mu_1^C|$, μ_1^C is the chemical potential of component 1 at the plait point, C_1 and $\tilde{C}_1$ are the component 1 concentrations in the two phases, and B_1 is a constant, the actual magnitude of which depends on the particular choice of units for C_1 (for example, mass fraction, mole fraction, etc.) β must be the usual coexistence curve exponent (Table 1), since μ_1, like temperature and pressure, is a field variable (Tisza, 1966; Griffiths and Wheeler, 1970), that is, one which is the same in two coexisting phases, and the critical exponents must be unchanged under transformations in field variable (Griffiths and Wheeler, 1970) space.

TABLE 1. SUMMARY OF DEFINITIONS AND VALUES FOR CRITICAL EXPONENTS

Exponent	Definition	Value	Quantity
α	$C_V \sim \lvert T - T_C\rvert^{-\alpha}$	1/8	Constant volume specific heat
β	$\rho_L - \rho_V \sim (T_C - T)^{\beta}$	5/16	Shape of coexistence curve
γ	$K_T \sim \lvert T - T_C\rvert^{-\gamma}$	5/4	Isothermal compressibility

Similarly, we have for the sum of concentrations

$$C_1 + \tilde{C}_1 = 2C_1^C + 2A_1\epsilon_1^{1-\alpha} \tag{3}$$

where $\alpha < 1$, and C_1^C is the concentration of component 1 at the plait point. That α is the specific heat exponent follows from the above-mentioned equivalence of field variables and that concentration and entropy are equivalent density variables (Griffiths and Wheeler, 1970), that is, quantities which are different in coexisting phases.

Because of the single degree of freedom of the ternary, two-phase system and the fact that the choice of the component labeled 1 was arbitrary, we must have relations similar to (2) and (3) for the other components as well,

$$C_2 - \tilde{C}_2 = B_2\epsilon_1^{\beta} \tag{4}$$

$$\overline{C}_2 - C_2^C = A_2\epsilon_1^{1-\alpha} \tag{5}$$

$$C_3 - \tilde{C}_3 = B_3\epsilon_1^{\beta} \tag{6}$$

and

$$\overline{C}_3 - C_3^C = A_3\epsilon_1^{1-\alpha} \tag{7}$$

where

$$\overline{C}_2 = \frac{C_2 + \tilde{C}_2}{2} \quad \text{and} \quad \overline{C}_3 = \frac{C_3 + \tilde{C}_3}{2}$$

Since the concentrations must be normalized to unity in each phase

$$C_1 + C_2 + C_3 = 1 \tag{8}$$

$$\tilde{C}_1 + \tilde{C}_2 + \tilde{C}_3 = 1 \tag{9}$$

the coefficients A_1, etc., and B_1, etc., are not independent. From (8) and (9) we must have

$$B_1 + B_2 + B_3 = 0 \tag{10}$$

and

$$A_1 + A_2 + A_3 = 0 \tag{11}$$

We can eliminate μ_1 as a variable in terms of $\overline{C}_1 = C_1 + \tilde{C}_1/2$, for example, to obtain

$$C_1 - \tilde{C}_1 = \overline{B}_1\lvert\overline{C}_1 - C_1^C\rvert^{\beta/(1-\alpha)} \tag{12}$$

$$C_2 - \tilde{C}_2 = \overline{B}_2\lvert\overline{C}_1 - C_1^C\rvert^{\beta/(1-\alpha)} \tag{13}$$

$$\overline{C}_2 - C_2^C = \overline{A}_2(\overline{C}_1 - C_1^C) \tag{14}$$

$$C_3 - \tilde{C}_3 = \overline{B}_3\lvert\overline{C}_1 - C_1^C\rvert^{\beta/(1-\alpha)} \tag{15}$$

and

$$\overline{C}_3 - C_3^C = \overline{A}_3(\overline{C}_1 - C_1^C) \tag{16}$$

where

$$\overline{B} = \frac{B_1}{\lvert A_1\rvert}\beta/(1-\alpha), \quad \overline{B}_2 = \frac{B_2}{\lvert A_2\rvert}\beta/(1-\alpha),$$

$$B_3 = \frac{B_3}{\lvert A_1\rvert}\beta/(1-\alpha), \quad \overline{A}_2 = \frac{A_2}{A_1}, \quad \text{and} \quad \overline{A}_3 = \frac{A_3}{A_1}$$

Consider a linear path through the ternary diagram defined by the composition coordinates $(\hat{C}_1, \hat{C}_3)$ satisfying

$$\hat{C}_1 - C_1^C = \delta\hat{C}_1 + M(\hat{C}_3 - \hat{C}_3^C) \tag{17}$$

where M is a constant. $\delta\hat{C}_1$ is a measure of the nearness that the path passes to the plait point; that is, it is the value of $\hat{C}_1 - C_1^C$ when $\hat{C}_3 = C_3^C$ (the actual distance of closest approach to the plait point can be shown to be $\delta\hat{C}_1/(M^2 + M + 1)$).

Suppose a point on the path (17) intersects a tie line determined by concentrations C_1, C_3 and $\tilde{C}_1$, $\tilde{C}_3$. The mass fraction of the C_1, C_3 phase is

$$F = \frac{\tilde{C}_1 - \hat{C}_1}{\tilde{C}_1 - C_1} \tag{18}$$

We can rewrite (18) in terms of $\overline{C}_1$ by noting that

$$\tilde{C}_1 = \tfrac{1}{2}(\tilde{C}_1 - C_1) + \tfrac{1}{2}(\tilde{C}_1 + C_1) = \overline{C}_1 + \tfrac{1}{2}(\tilde{C}_1 - C_1) \tag{19}$$

Thus

$$F = \tfrac{1}{2} + \frac{\overline{C}_1 - \hat{C}_1}{\tilde{C}_1 - C_1} = \tfrac{1}{2} + \frac{\overline{C}_1 - C_1^C + C_1^C - \hat{C}_1}{\tilde{C}_1 - C_1}$$

$$= \tfrac{1}{2} + \frac{\overline{C}_1 - C_1^C + C_1^C - \hat{C}_1}{\overline{B}_1\lvert\overline{C}_1 - C_1^C\rvert^{\beta/(1-\alpha)}} \tag{20}$$

The equation for the tie line intersected by $\hat{C}_1$, $\tilde{C}_3$ requires that

$$\hat{C}_1 - \tilde{C}_1 = \frac{\tilde{C}_1 - C_1}{\tilde{C}_3 - C_3}(\hat{C}_3 - \tilde{C}_3) = \frac{\overline{B}_1}{\overline{B}_3}(\hat{C}_3 - \tilde{C}_3) \tag{21}$$

which also can be written as

$$C_1 - \hat{C}_1 = \frac{\overline{B}_1}{\overline{B}_3}(C_3 - \hat{C}_3) \tag{22}$$

Thus

$$\hat{C}_1 - C_1^C = \hat{C}_1 - \overline{C}_1 + \overline{C}_1 - C_1^C$$

$$= \frac{\overline{B}_1}{\overline{B}_3}(\hat{C}_3 - \overline{C}_3) + \overline{C}_1 - C_1^C \tag{23}$$

$$= \frac{\overline{B}_1}{\overline{B}_3}[\hat{C}_3 - C_3^C - \overline{A}_3(\overline{C}_1 - C_1^C)] + \overline{C}_1 - C_1^C)$$

$$= \left(1 - \frac{\overline{B}_1}{\overline{B}_3}\overline{A}_3\right)(\overline{C}_1 - C_1^C) + \frac{\overline{B}_1}{\overline{B}_3}(\hat{C}_3 - C_3^C)$$

where we have used (16).

Equating the right-hand side of (23) with that of (17) allows us to solve for $\overline{C}_1 - C_1^C$ in terms of $\hat{C}_3 - C_3^C$ to obtain

$$\overline{C}_1 - C_1^C = \frac{\delta\hat{C}_1 + \left(M - \frac{\overline{B}_1}{\overline{B}_3}\right)(\hat{C}_3 - C_3^C)}{1 - \frac{\overline{B}_1}{\overline{B}_3}\overline{A}_3} \tag{24}$$

Substitution of (24) into (20) yields, after some manipulation

$$F = \tfrac{1}{2} - \frac{\left|1 - \frac{\overline{B}_1}{\overline{B}_3}\overline{A}_3\right|^{\beta/(1-\alpha)}}{\overline{B}_3\left(1 - \frac{\overline{B}_1}{\overline{B}_3}\overline{A}_3\right)} \left[\frac{\delta\hat{C}_1\overline{A}_3 + (M\overline{A}_3 - 1)(\hat{C}_3 - C_3^C)}{\left|\delta\hat{C}_1 + \left(M - \frac{\overline{B}_1}{\overline{B}_3}\right)(\hat{C}_3 - C_3^C)\right|^{\beta/(1-\alpha)}}\right] \tag{25}$$

Equation (25) can be rewritten as

$$F = \tfrac{1}{2} - \left|\frac{1 - \overline{B}_1\overline{A}_3/\overline{B}_3}{M - \overline{B}_1/\overline{B}_3}\right|^{\beta/(1-\alpha)} \cdot \frac{\delta\hat{C}_1\overline{A}_3 + (M\overline{A}_3 - 1)(\hat{C}_3 - C_3^C)}{(\overline{B}_3 - \overline{B}_1\overline{A}_3)|\hat{C}_3 - C_3^o|^{\beta/(1-\alpha)}} \tag{26}$$

where

$$C_3^o = C_3^C - \frac{\delta\hat{C}_1}{M - \frac{\overline{B}_1}{\overline{B}_3}}$$

This can be rewritten as

$$F = \tfrac{1}{2}\left\{1 - \left|\frac{\overline{C}_3^o - C_3^o}{\hat{C}_3 - C_3^o}\right|^{\beta/(1-\alpha)} \cdot [1 + \lambda(\hat{C}_3 - \overline{C}_3^o)]\right\} \tag{27a}$$

if

$$\frac{\delta\hat{C}_1\overline{A}_3 + (M\overline{A}_3 - 1)(C_3^o - C_3^C)}{\overline{B}_3 - \overline{B}_1\overline{A}_3} > 0 \quad \text{(case I)}$$

or

$$F = \tfrac{1}{2}\left\{1 + \left|\frac{\overline{C}_3^o - C_3^o}{\hat{C}_3 - C_3^o}\right|^{\beta/(1-\alpha)} [1 + \lambda(\hat{C}_3 - \overline{C}_3^o)]\right\} \tag{27b}$$

if

$$\frac{\delta\hat{C}_1\overline{A}_3 + (M\overline{A}_3 - 1)(C_3^o - C_3^C)}{\overline{B}_3 - \overline{B}_1\overline{A}_3} < 0 \quad \text{(case II)}$$

where

$$\lambda = \frac{M\overline{A}_3 - 1}{\delta\hat{C}_1\overline{A}_3 + (M\overline{A}_3 - 1)(\overline{C}_3^o - C_3^C)}$$

and $\overline{C}_3^o$ is the solution to

$$\frac{|\overline{C}_3^o - C_3^o|^{\beta/(1-\alpha)}}{\delta\hat{C}_1\overline{A}_3 + (M\overline{A}_3 - 1)(\overline{C}_3^o - C_3^C)} = \frac{\pm 2}{\overline{B}_3 - \overline{B}_1\overline{A}_3}\left|\frac{1 - \overline{B}_1\overline{A}_3/\overline{B}_3}{M - \overline{B}_1/\overline{B}_3}\right|^{\beta/(1-\alpha)} \tag{28}$$

The plus sign applies for case I and the minus sign applies for case II.

Let us examine the structure of Equations (27). Equation (27*a*) says that the phase having concentrations C_1 and C_3 disappears when $\hat{C}_3 = \overline{C}_3^o$. If $|\overline{C}_3^o - C_3^o|$ is very small, then the phase disappears very rapidly as a function of $\hat{C}_3$, while if $|\overline{C}_3^o - C_3^o|$ is relatively large, then the phase disappears gradually as a function of $\hat{C}_3$. As we shall see, the former case corresponds to a path which passes very close to the plait point, while the latter case corresponds to a path which passes relatively far from the plait point. To see this we note that for sufficiently small $\delta\hat{C}_1$, (28) can be approximated by

$$|\overline{C}_3^o - C_3^o|^{\beta/(1-\alpha)} \simeq \pm 2\frac{\delta\hat{C}_1\overline{A}_3 + (M\overline{A}_3 - 1)(C_3^o - C_3^C)}{\overline{B}_3 - \overline{B}_1\overline{A}_3}\left|\frac{1 - \overline{B}_1\overline{A}_3/\overline{B}_3}{M - \overline{B}_1/\overline{B}_3}\right|^{\beta/(1-\alpha)} \tag{29}$$

$$= \pm\,\delta\hat{C}_1\frac{\overline{A}_3 - (M\overline{A}_3 - 1)/(M - \overline{B}_1/\overline{B}_3)}{\overline{B}_3 - \overline{B}_1\overline{A}_3}\left|\frac{1 - \overline{B}_1\overline{A}_3/\overline{B}_3}{M - \overline{B}_1/\overline{B}_3}\right|^{\beta/(1-\alpha)}$$

Thus, $|\overline{C}_3^o - C_3^o|$ is small if $\delta\hat{C}_1$ is small, that is, a path

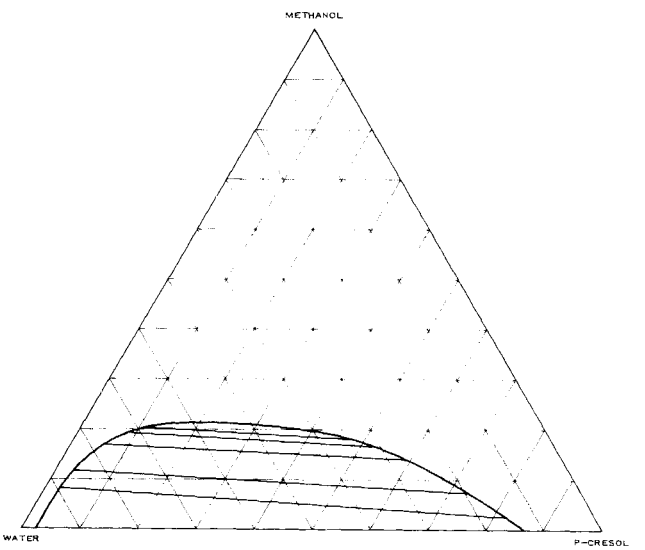

Fig. 1. Ternary phase diagram for water-methanol-p-cresol at 35°C. Data from Prutton et al. (1950).

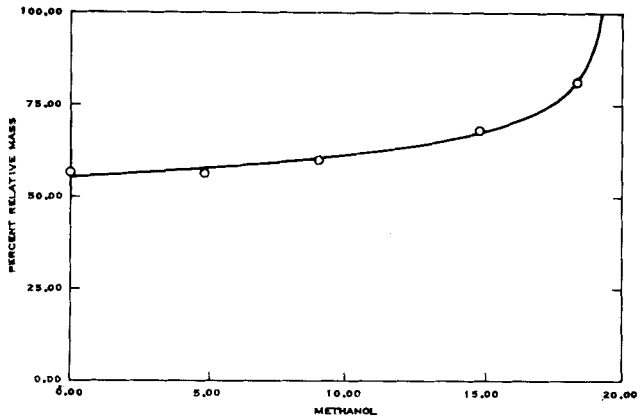

Fig. 2. Phase mass diagram for water-methanol-*p*-cresol as a function of methanol concentration for equal masses of water and *p*-cresol.

passing very close to the plait point. We'll see how this is manifest with some actual experimental phase volume diagrams later.

There is one limiting case which is not readily apparent from the explicit form of (27). If $M = \overline{B}_1/\overline{B}_3$, that is, a path which is coincident with a tie line, then C_3^o diverges. Then (27*a*) and (27*b*) become

$$F = -\frac{\lambda}{2}(\hat{C}_3 - \overline{C}_3^o) \quad \text{(case I)} \qquad (30a)$$

and

$$F = 1 + \frac{\lambda}{2}(\hat{C}_3 - \overline{C}_3^o) \quad \text{(case II)} \qquad (30b)$$

This is the expected result that the phase volume along a tie line is a linear function of the distance along that tie line. For this situation, the equations for λ and $\overline{C}_3^o$ reduce to

$$\lambda = -\left| \frac{1 - \overline{B}_1\overline{A}_3/\overline{B}_3}{\delta\hat{C}_1} \right|^{\beta/(1-\alpha)} \qquad (31)$$

and

$$\overline{C}_3^o - C_3^C = \tfrac{1}{2}\left| \frac{\delta\hat{C}_1}{1 - \overline{B}_1\overline{A}_3/\overline{B}_3} \right|^{\beta/(1-\alpha)} - \delta\hat{C}_1\overline{A}_3$$

$$= -1/(2\lambda) - \delta\hat{C}_1\overline{A}_3 \qquad (32)$$

Thus, λ is very large for tie lines near the plait point, while $\overline{C}_3^o - C_3^C$ is still small for such tie lines.

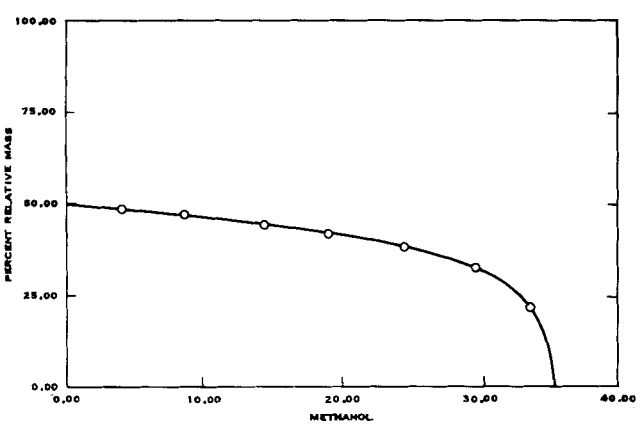

Fig. 4. Phase mass diagram for water-methanol-methylmethacrylate as a function of methanol concentration for equal masses of water and methyl methacrylate.

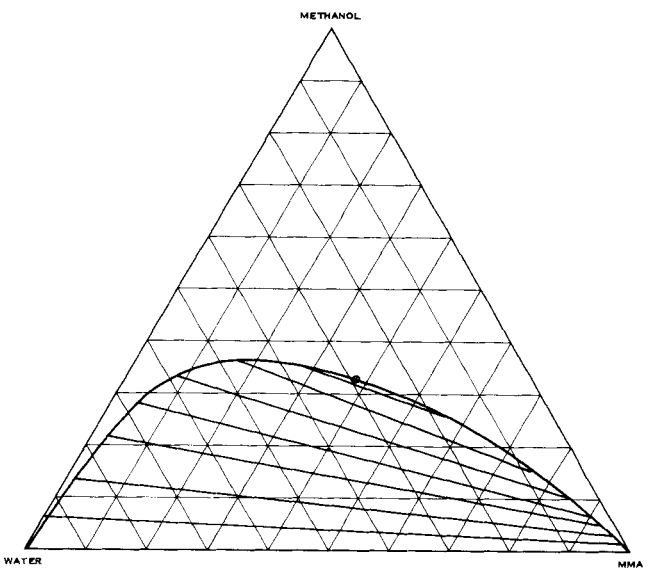

Fig. 3. Ternary phase diagram for water-methanol-methylmethacrylate at 25°C. Data from Kooi (1949).

COMPARISON WITH EXPERIMENTS IN TERNARY SYSTEMS

In this section, we will show that Equations (27) can be used to fit phase volume diagrams in ternary systems. Since the choice of the component labeled 3 in Equations (27) was arbitrary, we will drop the subscript. We need consider (27*a*), since (27*b*) can be obtained by subtracting (27*a*) from unity. Thus, when a composition C is expressed as mass fraction, the corresponding mass fraction of the disappearing phase is

$$F = \tfrac{1}{2}\left\{1 - \left(\frac{\overline{C}^o - C^o}{C - C^o}\right)^{\beta/(1-\alpha)}[1 + \lambda(C - \overline{C}^o)]\right\} \qquad (33)$$

Sufficiently near the plait point, the volume fraction will also be given by (33), since the densities of both phases approach one another at the plait point. It should be sufficiently accurate to take $\beta = 5/16$ and $\alpha = \frac{1}{8}$ (see Table 1).

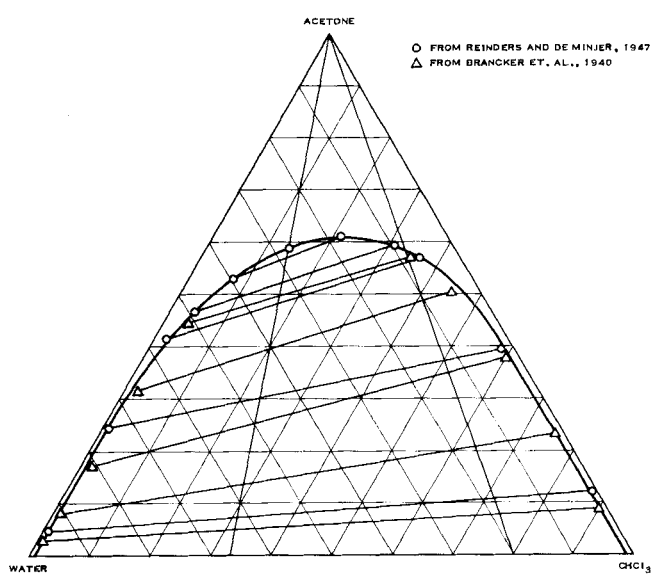

Fig. 5. Ternary phase diagram for water-chloroform-acetone at 25°C. The two paths shown are the ones chosen for calculation of phase mass diagrams. Data from Reinders and DeMinjer (1947) and Brancker et al. (1940).

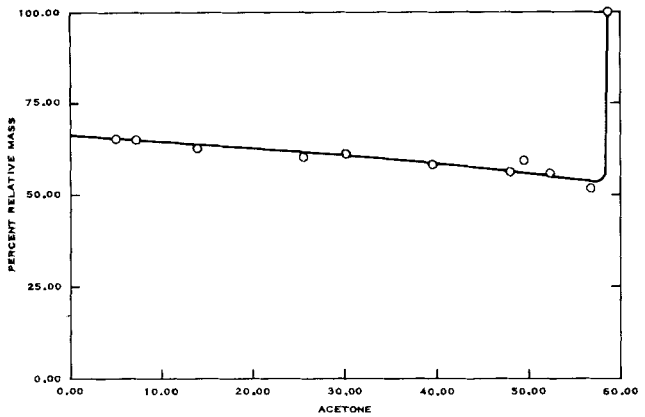

Fig. 6. Phase mass diagram for water-chloroform-acetone at 25°C as a function of acetone concentration for a 2:1 ratio of water to chloroform.

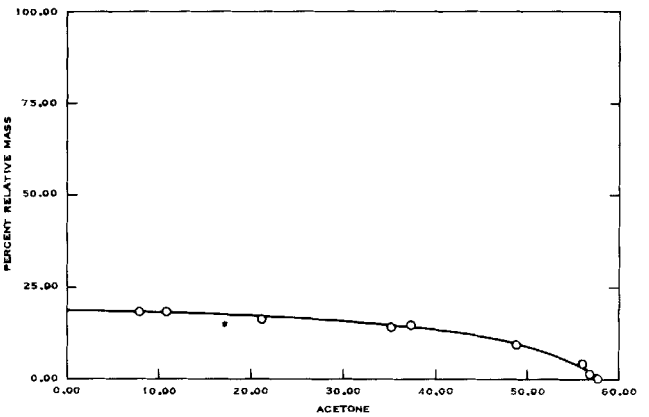

Fig. 7. Same as Figure 6 for a 1:4 ratio of water to chloroform.

Consider, for example, the ternary phase diagram at 25°C for the system water-*p*-cresol-methanol (Prutton et al., 1950) (Figure 1). The mass fractions of the phases for a given path through the diagram can be calculated from the point of intersection with the experimental tie lines. The calculated mass fractions for equal masses of water and *p*-cresol as a function of methanol concentration are shown in Figure 2 (in analogy with the phase volume diagram, this plot should be called a phase mass diagram). The smooth curve was obtained from Equation (33) with $C^o = 0.1910$, $\overline{C^o} = 0.1890$, and $\lambda = 2.92$. These values for the parameters were obtained using a modification of Bevington's (1969) nonlinear, least-square subroutine CURFIT.

A similarly excellent fit can be obtained for the ternary system water-methanol-methylmethacrylate (Kooi, 1949) at 25°C (Figure 3). For equal masses of water and methylmethacrylate, the mass fractions as a function of methanol concentration (Figure 4) can be fit with $C^o = 0.3596$, $\overline{C^o} = 0.3542$, and $\lambda = 2.77$. The fit again is excellent.

Let us consider in more detail another ternary system, water-acetone-chloroform (Reinders and De Minjer, 1947; Brancker et al., 1940) at 25°C. We consider two paths in the phase diagram shown in Figure 5. One, corresponding to a water to chloroform ratio of 2:1, passes very close to the plait point, while the other, corresponding to a water to chloroform ratio of 1:4, does not pass so near to the plait point. This behavior is reflected in the corresponding phase mass diagrams shown in Figures 6 and 7. For the 2:1 line, the solid curve was obtained with $C^o = 0.5864008$, $\overline{C^o} = 0.5863980$, and $\lambda = -42.4$, while for the 1:4 line, the fit was obtained with $\overline{C^o} = 0.6690$, $\overline{C^o} = 0.5799$, and $\lambda = -0.503$. The closeness to the plait point of the former path is reflected in the extremely small value of $C^o - \overline{C^o} = 2.8 \times 10^{-6}$ compared with the larger value of $C^o - \overline{C^o} = 0.0891$ for the latter path.

It is actually possible to calculate values for these fit parameters using Equations (26), (27), and (28). By a least-squares fit to the four tie lines closest to the plait point in Figure 5, we obtain

$$\overline{A_3} = -2.59 \pm 0.73 \qquad (34a)$$

$$\overline{B_1} = -1.52 \pm 0.22 \qquad (34b)$$

and

$$\overline{B_3} = 0.47 \pm 0.11 \qquad (34c)$$

The tolerances are the standard deviations for the corresponding parameters. Substituting these values into the expressions for the parameters, we get

$$C^o = 0.5861 \pm 0.0001 \qquad (35a)$$

$$C^o - \overline{C^o} = (0.50 \pm 0.28) \times 10^{-6} \qquad (35b)$$

and

$$\lambda = -108 \pm 27 \qquad (35c)$$

for the 2:1 water-chloroform path ($M = -2/3$) and

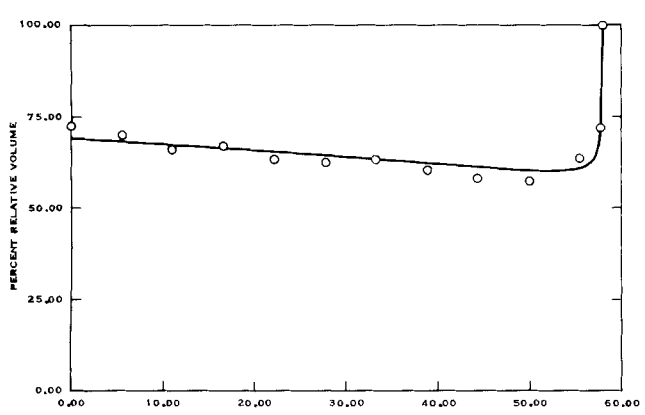

Fig. 8. Experimental phase volume diagram for water-chloroform-acetone at room temperature as a function of acetone concentration for a 2:1 ratio of water to chloroform.

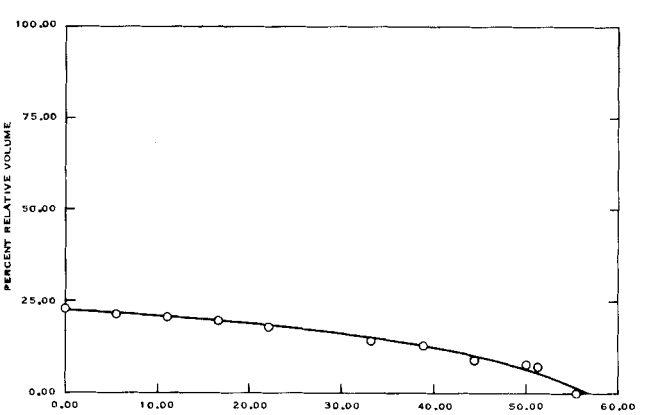

Fig. 9. Same as Figure 6 for a 1:4 ratio of water to chloroform.

$$C^o = 0.650 \pm 0.006 \qquad (36a)$$

$$C^o - \overline{C}^o = 0.074 \pm 0.040 \qquad (36b)$$

and

$$\lambda = -1.03 \pm 0.55 \qquad (36c)$$

for the 1:4 water-chloroform path.

The values obtained from the least-squares fits to the phase mass diagrams are within the tolerances for all cases except for (35*b*) and (35*c*). The deviations in those cases are not so severe when we note that these values were obtained using $\delta\hat{C}_1 = 0.0023$ based on the experimental (Brancker et al., 1940) plait point coordinates $C^c_{H_2O} = 0.273$, $C^c_{CHCl_3} = 0.140$ and $C^c_{acetone} = 0.587$. An error by a factor of 2 in $\delta\hat{C}_1$, which corresponds to an error in the plait point composition of only 0.001, is all that is needed to obtain agreement within the tolerances. In light of this sensitivity to the estimated plait point composition, the agreement of the calculated and least-squares fit parameters must be considered very good.

In order to confirm this behavior, we have experimentally determined phase volume diagrams for the same two lines in this system (Figures 8 and 9). These were done at room temperature (~26°C), and, hence, perfect agreement should not be expected. Nevertheless, despite this and the fact that volumes instead of mass fractions were measured, the two curves are very similar to those determined from the experimental tie lines. For the 2:1 line, the best fit was obtained with $C^o = 0.58019$, $\overline{C}^o = 0.58000$, and $\lambda = -9.8$, while for the 1:4 line, the fit was obtained with $C^o = 0.7006$, $\overline{C}^o = 0.5650$, and $\lambda = 0.018$. These yield $C^o - \overline{C}^o = 0.00019$ and $C^o - \overline{C}^o = 0.1356$, respectively. The relative distance to the critical point should be about

$$\left(\frac{0.1356}{0.00019}\right)^{5/14} \simeq 10 \qquad (37)$$

which is the same order of magnitude as the value of 41 which would be obtained from a fit to the tie lines at 25°C.

Overall, we must regard the agreement with the theoretical Equation (31) to be excellent. If we consider the limited range of validity of the derivation, that is, treat only behavior very near the critical point, it is remarkable that this equation can describe the experimental phase volume (or phase mass) diagrams over such a wide range of compositions.

PHASE VOLUME DIAGRAMS IN SURFACTANT SYSTEMS

We wish to generalize Equation (31) so as to include systems of three fluid phases, since such systems have been seen to be effective in tertiary oil recovery (Boneau and Clampitt, 1977; Healy and Reed, 1977). For a three-phase system, a critical end point is analogous to a plait point in a two-phase system. A critical end point is a point on the phase diagram at which two phases become critical in the presence of a third. Such a point is, nevertheless, a second-order critical point and should, therefore, have the same critical exponents as an ordinary critical point. Hence, the exponent $\beta/(1-\alpha)$ should occur in the generalized equation in a manner similar to that in (33).

The multiplicative factor of ½ in front of the bracket in Equation (33) resulted from the fact that two phases become critical at the plait point. For a three-phase system, the amount of third phase can be chosen arbitrarily without changing the nature of the two near-

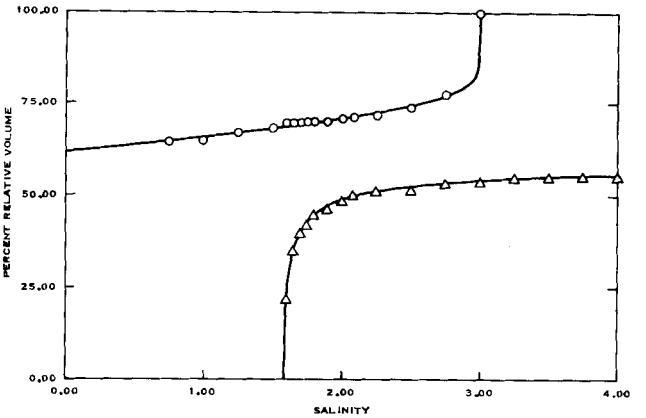

Fig. 10. Experimental phase volume diagram for surfactant system containing 1.98% sodium sulfonate extracted from Witco TRS 10-410 petroleum sulfonate 1.98% isobutyl alcohol, 62.04% brine and 34% 1-phenyltetradecane as a function of salinity of the brine.

critical phases. Therefore, the simplest generalization of Equation (19) is of the form

$$F = F_o\left[1 - \left(\frac{\overline{C}^o - C^o}{C - C^o}\right)^{\beta/(1-\alpha)}(1 + \lambda(C - \overline{C}^o)\right] \qquad (38)$$

F_o will be taken as an adjustable constant to be determined by the method of least squares along with $\overline{C}^o$, C^o, and λ.

In order to test this equation, we consider the phase volume diagram generated by the set of systems formed by mixing 66 wt % aqueous surfactant system, containing 3 wt % sodium sulfonate extracted from Witco TRS 10-410 petroleum sulfonate, 3 wt % isobutyl alcohol, and 92% brine, with 34 wt % of 1-phenyltetradecane. The phase volumes are then plotted vs. salinity of the brine (Figure 10). This diagram has two branches, since there is a three-phase region for intermediate salinities. It is not possible to depict the associated phase diagram for this system which contains five components, since a four-dimensional figure is required for full representation (Vinatieri and Fleming, 1978). The solid curve obtained by least-squares fit to the top phase volume was obtained with $F_o = 0.2219$, $\overline{C}^o = 0.03000$, $C^o = 0.03001$, and $\lambda = 466.7$. Similarly, the volume of the bottom phase was fit with $F_o = 0.6565$, $\overline{C}^o = 0.01580$, $C^o = 0.01571$, and $\lambda = 3.87$. The fits are excellent for both branches.

Similarly, the phase volume diagrams with decane, tetradecane, and hexadecane substituted for 1-phenyltetradecane are shown in Figures 11, 12, and 13, respectively (Glinsmann, 1977). The fit parameters for these curves are summarized in Table 2.

The fits to the experimental phase volume diagrams in surfactant systems are excellent in all cases. It is of interest to note that as the alkane carbon number (Cash et al., 1976; Cayias et al., 1976) of the hydrocarbon increases, the phase volume diagram passes nearer to the oil-microemulsion critical end point. For example, the tetradecane diagram passes about

$$\left(\frac{1.2 \times 10^{-3}}{1.1 \times 10^{-7}}\right)^{5/14} \simeq 28 \qquad (39)$$

times closer than does the decane diagram. The hexadecane diagram passes even closer, approximately

$$\left(\frac{1.2 \times 10^{-3}}{2.2 \times 10^{-10}}\right)^{5/14} \simeq 250 \qquad (40)$$

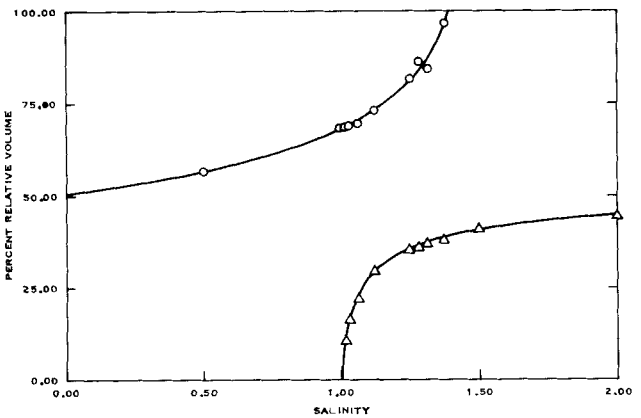

Fig. 11. Experimental phase volume diagram as a function of salinity for surfactant system consisting of 24 ml of brine and 26 ml of a solution containing 1 g of sodium sulfonate extracted from Witco TRS 10-410 petroleum sulfonate, 1 g of isobutyl alcohol and decane.

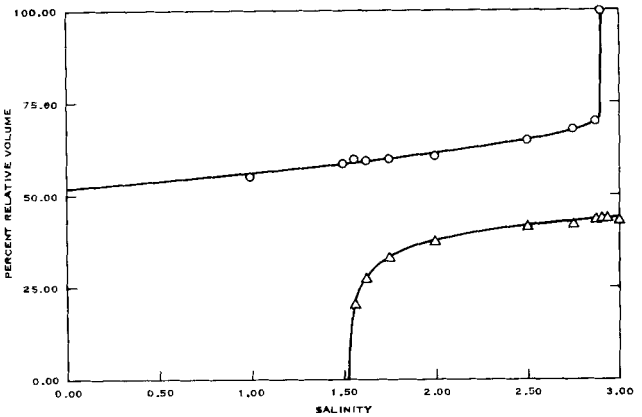

Fig. 12. Same as Figure 11 except with tetradecane as the oil.

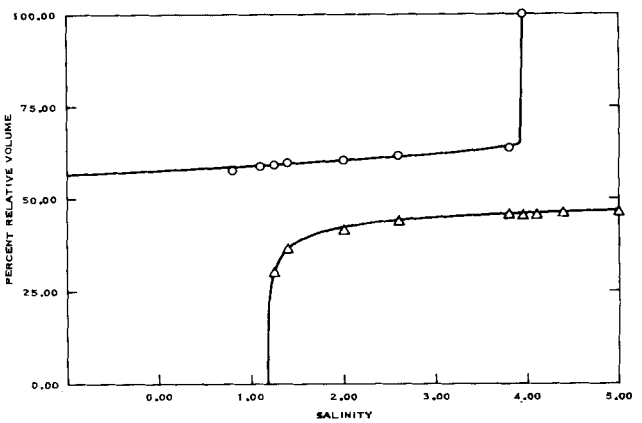

Fig. 13. Same as Figure 11 except with hexadecane as the oil.

times closer. By contrast, the phenyltetradecane diagram only passes about

$$\left(\frac{1.2 \times 10^{-3}}{9.1 \times 10^{-6}}\right)^{5/14} \simeq 6 \qquad (41)$$

times closer than does the decane diagram.

No such wide variation was observed in the distances of the phase volume diagrams from the corresponding water phase-microemulsion critical end points. The respective distances for decane, tetradecane, phenyltetradecane, and hexadecane are approximately in the ratio

$$(2.4 \times 10^{-4})^{5/14}:(1.15 \times 10^{-4})^{5/14}:(9.0 \times 10^{-5})^{5/14}:$$
$$(6.5 \times 10^{-5})^{5/14} = 1:.77:.70:.63$$

that is, they all pass about the same distance from the critical end points.

DISCUSSION

We have seen that the shapes of phase volume diagrams can be indicative of the nearness to critical points. We have been able to quantify this dependence by making use of modern theory of critical phenomena. For phase volume diagrams which pass near to critical points, the volume of one of the phases goes rapidly to zero for a small change in concentration.

For a ternary, two-phase system, we have shown that a phase volume diagram can be described in terms of three parameters. One is the concentration at which a phase disappears, another measures the nearness to criticality, and a third is necessary to allow for paths which are nearly parallel to tie lines. The resulting equation was seen to yield excellent agreement with phase volume (and phase mass) diagrams obtained both by direct experiment and by calculation from experimental tie lines. For a particular system, water-chloroform-acetone, the values of the parameters obtained from a least-squares fit were in reasonable agreement with those calculated from a fit to the experimental tie lines.

For multicomponent systems where a third phase may be present, it is necessary to introduce an additional parameter. This parameter is essentially a scale factor which is required because an arbitrary amount of a third phase can be present in a system without altering the nature of two near critical phases. With the inclusion of this additional parameter, excellent agreement was

Table 2. Fit Parameters for Surfactant Systems

Oil	F^o	C^o	$\bar{C}^o$	$\lvert C^o - \bar{C}^o \rvert$	λ
1-phenyltetradecane					
Upper phase	0.222	0.03001	0.03000	0.91×10^{-5}	467
Lower phase	0.656	0.01571	0.01580	0.9×10^{-4}	3.87
Decane					
Upper phase	0.708	0.0151	0.0139	0.0012	17.9
Lower phase	0.620	0.00974	0.00998	2.4×10^{-4}	5.63
Tetradecane					
Upper phase	0.307	0.02906	0.02906	1.1×10^{-7}	1 736
Lower phase	0.489	0.01510	0.01521	1.15×10^{-4}	−29.8
Hexadecane					
Upper phase	0.350	0.04125	0.04125	2.2×10^{-10}	5.331
Lower phase	0.517	0.01797	0.01804	6.5×10^{-5}	−3.93

obtained between the theoretical equation and experimental phase volume diagrams in three-phase surfactant systems.

Phase volume diagrams have proven to be a useful tool in characterizing surfactant oil recovery systems. With the methods developed here, the utility of these diagrams can be increased, and they can become a quantitative aid in the evaluation of surfactant systems. The derivation of a relationship between interfacial tension and phase volumes should be possible using the methods presented here.

SUMMARY AND CONCLUSIONS

This study of phase volume diagrams and their relationship to critical behavior has increased our understanding of these diagrams and should extend their utility for the study of surfactant systems for tertiary oil recovery. The specific conclusions of this work are as follows:

1. A three-parameter equation has been developed for two-phase systems.
2. A four-parameter equation has been developed for three-phase systems.
3. These equations can be used to quantify the distance from the path of the phase volume diagram to the appropriate critical point(s).
4. For three-phase surfactant systems, the phase volume diagram approaches the oil-microemulsion critical end point as the alkane carbon number of the oil is increased.

NOTATION

A_1 = proportionality constant in Equation (3)
A_2 = proportionality constant in Equation (5)
A_3 = proportionality constant in Equation (7)
$\overline{A}_2$ = A_2/A_1
$\overline{A}_3$ = A_3/A_1
B_1 = proportionality constant in Equation (2)
B_2 = proportionality constant in Equation (4)
B_3 = proportionality constant in Equation (6)
$\overline{B}_1$ = $B_1/|A_1|^{\beta/(1-\alpha)}$
$\overline{B}_2$ = $B_2/|A_1|^{\beta/(1-\alpha)}$
$\overline{B}_3$ = $B_3/|A_1|^{\beta/(1-\alpha)}$
$C_1, \tilde{C}_1$ = concentrations of component labeled 1 in coexisting phases
$C_2, \tilde{C}_2$ = concentrations of component labeled 2 in coexisting phases
$C_3, \tilde{C}_3$ = concentrations of component labeled 3 in coexisting phases
C_1^C, C_2^C, C_3^C = plait point compositions of components 1, 2, and 3, respectively
$\overline{C}_1$ = $C_1 + \tilde{C}_1/2$
$\overline{C}_2$ = $C_2 + \tilde{C}_2/2$
$\overline{C}_3$ = $C_3 + \tilde{C}_3/2$
$\hat{C}_1, \hat{C}_3$ = composition pairs along path in ternary diagram
$\delta\hat{C}_1$ = value of $\hat{C}_1 - C_1^C$ when $\hat{C}_3 = C_3^C$
C_3^o = $C_3^C - \delta\hat{C}_1/(M - \overline{B}_1/\overline{B}_3)$
$\overline{C}^o$ = solution of Equation (28)
$\overline{C}^o, C^o$ = parameters in Equation (33)
C = concentration being varied in phase volume diagram
d = degree of binodal curve
F = fraction of disappearing phase
F_o = proportionality constant in equation
i = index labeling components
K_T = $-1/V(\partial V/\partial P)_T$ = isothermal compressibility
M = slope in Equation (17)
P = pressure
T = temperature
T_C = critical temperature
V = volume

Greek Letters

α = specific heat exponent, defined in Table 1
β = coexistence curve exponent, defined in Table 1
γ = compressibility exponent, defined in Table 1
ϵ_1 = $|(\mu_1 - \mu_1^C)/\mu_1^C|$
λ = parameter defined in Equation (27)
μ_1 = chemical potential of component labeled 1
μ_1^C = value of μ_1 at the plait point
ρ_L, ρ_V = liquid and vapor densities, respectively

LITERATURE CITED

Bevington, P. R., *Data Reduction and Error Analysis for the Physical Sciences*, pp. 237-242, McGraw-Hill, New York (1969).

Boneau, D., and R. Clampitt, "A Surfactant System for the Oil-Wet Sandstone of the North Burbank Unit," *J. Petrol. Technol.*, 501-506 (May, 1977).

Brancker, A. V., T. G. Hunter, and A. W. Nash, "The Quaternary System Acetic Acid-Chloroform-Acetone-Water at 25 C," *J. Phys. Chem.*, **44**, 683 (1940).

Cash, R. L., J. L. Cayias, R. G. Fournier, J. K. Jacobson, T. Schares, R. S. Schechter, and W. H. Wade, "Modeling Crude Oils for Low Interfacial Tension," SPE 5813, SPE Symposium on Improved Oil Recovery, Tulsa, Okla. (Mar. 22-24, 1976).

Cayias, J. L., W. H. Wade, and R. S. Schechter, "Modeling Crude Oils for Low Interfacial Tension," (a revision of SPE 5813), *SPE Journal*, **16**, 351 (1976).

Clark, R., and G. A. Neece, "Decorated Lattice Model for Ternary Systems," *J. Chem. Phys.*, **48**, 2575 (1968).

Fisher, M., "Renormalization of Critical Exponents by Hidden Variables," *Phys. Rev.*, **176**, 257 (1968).

Fleming, P. D., R. E. Terry, D. M. Sitton, J. E. Hessert, J. E. Vinatieri, and D. F. Boneau, "Phase Properties of Oil Recovery Systems Containing Petroleum Sulfonates," *SPE 7576*, paper presented at the 53rd Annual Technical Conference and Exhibition of the SPE in Houston, Tex. (Oct. 1-4, 1978).

Glinsmann, G. R., unpublished, has measured phase-volume diagrams for the decane, tetradecane, and hexadecane systems (1977).

Greer, S., "Coexistence Curves at Liquid-Liquid Critical Points: Ising Exponents and Extended Scaling," *Phys. Rev.*, **A14**, 1770 (1976).

Griffiths, R. B., and J. C. Wheeler, "Critical Points in Multicomponent Systems," *ibid.*, **A2**, 1047 (1970).

Healy, R. N., and R. L. Reed, "Immiscible Microemulsion Flooding," *SPE Journal*, **17**, 129 (1977).

Hockner, R., and M. R. Moldover, "Ising Critical Exponents in Real Fluids: An Experiment," *Phys. Rev. Letters*, **37**, 29 (1976).

Kooi, J., "The System Methyl Methacrylate-Methanol-Water," *Rec. Trav. Chim.*, **68**, 34 (1949).

Prutton, C. F., T. J. Walsh, and A. M. Desai, "Solvent Extraction of Tar Acids from Coal Tar Hydrocarbons," *Ind. Eng. Chem.*, **42**, 1210 (1950).

Reinders, W., and C. H. DeMinjer, "Vapor-Liquid Equilibrium in Ternary Systems, VI, The System Water-Acetone-Chloroform," *Rec. Trav. Chim.*, 66, 573 (1947).

Stanley, H. E., *Introduction to Phase Transitions and Critical Phenomena*, Oxford University Press, New York (1971).

Tisza, L., *Generalized Thermodynamics*, MIT Press, Cambridge, Mass. (1966).

Vinatieri, J., "Correlation of Emulsion Stability with Phase Behavior in Surfactant Systems for Tertiary Oil Recovery," submitted to an *SPE Journal* (1977).

———, and P. D. Fleming, "Use of Pseudocomponents in the Representation of Phase Behavior of Surfactant Systems," *SPE 7057*, paper presented at the Fifth Symposium on Improved Oil Methods of Oil Recovery, Tulsa, Okla. (Apr. 16-19, 1978).
Widom, B., "Plait Points in Two- and Three-Component Liquid Mixtures," *J. Chem. Phys.*, 46, 3324 (1967).
Zollweg, J., "Shape of the Coexistence Curve near a Plait Point in a Three-Component System," *ibid.*, 55, 1430 (1971).

Manuscript received October 18, 1977; revision received January 2, 1979 and accepted February 6, 1979.

Concentration Forcing of Catalytic Surface Rate Processes

MICHAEL B. CUTLIP

**Department of Chemical Engineering
Institute of Materials Science
The University of Connecticut
Storrs, Connecticut 06268**

Periodic feed switching between carbon monoxide/argon and oxygen/argon mixtures to a gradientless reactor has been found to significantly increase the average reaction rate as compared to the steady state rate, when the time averaged feed concentrations in both cases are stoichiometric. The rate enhancement achieved during periodic reactor operation is attributed to the attainment of more desirable surface concentrations on the platinum catalyst which dramatically increase the surface rate processes leading to carbon dioxide production.

Part I. Isothermal Carbon Monoxide Oxidation Over Supported Platinum

SCOPE

Most studies of chemical processes are made with the tacit assumption that steady state operation is optimal. Several researchers, notably Douglas (1972) and Bailey (1973, 1977) and their co-workers, have championed the potential benefits from the deliberate periodic or unsteady operation of chemical processes such as chemical reactions. Successful periodic operation capitalizes on the nonlinear nature of the process. Good candidates for periodic operation are catalytic reactions where increases in reaction rates and selectivities may occur when some combination of reactor temperature, feed concentration, or flow rate is varied. Increasing attention is being given to the fundamental surface rate processes in recent experimental studies into the periodic forcing of catalytic reactions.

In this work, the catalytic oxidation of carbon monoxide by a supported platinum catalyst was studied under isothermal conditions, where the reactor feed was alternated between an oxygen/argon mixture and a carbon monoxide/argon mixture. Gradientless reactor operation was used to eliminate potentially undesirable heat and mass transfer resistances so that the effects of the feed cycling on the intrinsic surface rate processes could be clearly observed.

CONCLUSIONS AND SIGNIFICANCE

Significant rate enhancement at constant temperature has been obtained for carbon monoxide oxidation over a supported platinum catalyst by the periodic introduction of the individual reactants to a gradientless reactor. This rate increase can be qualitatively explained by reference to the elementary surface steps commonly associated with this reaction, where the periodic feed forcing achieves surface coverages of adsorbed species which lead to increased rates of surface reaction.

For stoichiometric carbon monoxide and oxygen feed mixtures, steady state reactor operation results in a catalyst which is almost completely covered by the more strongly adsorbed carbon monoxide leaving small surface oxygen concentrations. Thus, the observed steady state reaction rate is low, since either of the proposed surface steps leading to product carbon dioxide is proportional to adsorbed atomic oxygen concentration. Since carbon monoxide and oxygen are quite irreversibly adsorbed while product carbon dioxide is not adsorbed, appropriate periodic operation can achieve a platinum catalyst containing both reactant species in such concentrations that the surface reactions as well as the adsorption rates of each reactant can occur so as to maximize the overall time averaged rate. In this periodic mode of operation, the surface rates leading to carbon dioxide serve to relieve the buildup of adsorbed carbon monoxide which otherwise would quench the high reaction rate.

These experimental results indicate that careful attention should be given to periodic processing where the catalytic surface rate processes can be significantly affected. Future work should indicate selectivity changes, as the concentrations of surface species can potentially be controlled by periodic operation. A detailed understand-